Machine visual motion detection modeled on vertebrate retina*

M. R. Blackburn, H. G. Nguyen and P. K. Kaomea

Naval Ocean Systems Center, Code 943
San Diego, California 92152-5000

ABSTRACT

Real-time motion analysis would be very useful for autonomous undersea vehicle (AUV) navigation, target tracking, homing, and obstacle avoidance. The perception of motion is well developed in animals from insects to man, providing solutions to similar problems. We have therefore applied a model of the motion analysis subnetwork in the vertebrate retina to visual navigation in the AUV. The model is currently implemented in the C programming language as a discrete- time serial approximation of a continuous-time parallel process. Running on an IBM-PC/AT with digitized video camera images, the system can detect and describe motion in a 16 by 16 receptor field at the rate of 4 updates per second. The system responds accurately with direction and speed information to images moving across the visual field at velocities less than 8 degrees of visual angle per second at signal-to-noise ratios greater than 3. The architecture is parallel and its sparse connections do not require long-term modifications. The model is thus appropriate for implementation in VLSI optoelectronics.

1. INTRODUCTION

The function of machine vision is to generate information on the relative location, change in location or movement, and distinguishing characteristics of objects in the visual field. For our purposes, this information will be used by an autonomous underwater vehicle in the performance of some physical work, such as navigation, search and recovery, or repair. To do so, the visual system must provide input and feedback to vehicle effector controllers. Additionally, autonomy dictates that the visual processing must take place on the vehicle, and a free-swimming vehicle requires that the visual processing take place in real time. To date, there have been few successes in the development of an on-board machine vision system that provides real-time analysis of motion for a moving vehicle.

In contrast to our difficulties with machine vision, most marine animals have solutions to vision requirements under water. These range from light sensitive spots that allow orienting, to complex retinal and cortical processing of form, color, and motion. The compound eyes of arthropods, including flies, beetles, lobsters and crabs, are designed primarily to detect motion [1], and while the vertebrate visual system has advanced pattern analysis across the phylogenetic scale, it has remained extremely sensitive to movement [2]. This suggests that motion analysis is a fundamental process in natural visual systems. Emulation of those natural processes may provide similar capabilities to artificial systems. We have therefore set out to explore the application of biological models to machine vision.

1.1 Motion analysis in the vertebrate retina

The neural connectivity of the vertebrate retina has been studied extensively [3,4,5,6], so there is much to draw upon in the construction of a model. It appears that visual systems are organized to perform two complimentary visual processes. One involves pattern and color, the other involves motion and spatial relationships [6,7]. The neural mechanisms of these two basic processes are evidently distinct in the retinal architecture and remain separable far into the cerebral cortex [8]. Motion analysis begins in the retina with a network involving rod receptors and transient-activity Y-type ganglion cells [9].

*Supported by the Department of the Navy. The opinions and assertions contained herein are those of the authors and are not to be construed as official of reflecting the views of the Department of the Navy. The motion analysis model described in this paper is the subject of a patent application.

SPIE Proc. 980: Underwater Imaging, San Diego, CA; pp. 82-89; 1988

Between the rods and Y-ganglion cells of the motion analysis subnetwork are beta horizontals, rod bipolars, and more than one type of amacrine cell [10]. A columnar segment of this subnetwork is shown schematically in Figure 1. The beta horizontals receive input from several rod receptors [10] and inhibit rod bipolars [11], The rod bipolars communicate with the two types of amacrine cells. The first type is a low density but large diameter receptive field cholinergic amacrine (A-I) interposed between the rod bipolar and Y-ganglion cells [12]. The second type of amacrine (A-II) has a higher density in the retina but each cell has a smaller diameter receptive field than the A-I amacrines. The neurotransmitter of the A-II amacrine is likely gama-aminobutyric acid (GABA), a known inhibitor. Pharmacological blockade of this neurotransmitter by picrotoxin was found to eliminate the null response of direction selectivity (defined in the next paragraph) in the rabbit retina [13]. Rod bipolars converge on the A-II amacrines with a ratio of about 30:1. It is possible that the A-II ama- crines inhibit the Y-ganglion cells, while the A-II amacrines themselves may be under inhibitory control from the rod bipolars [14,15]. Masland, Mills and Cassidy [16] suggest that despite the large dendritic field of cholinergic (A-I) amacrine cells, their output is localized to the immediate region surrounding the bipolar input. Since the dendrites of the ganglion cells extend into the inner plexiform layer and intermingle with bipolar axon arborizations and amacrine dendritic arborizations, both types of amacrine cells have the opportunity for local control over bipolar to ganglion transmission.

1.2 Direction selectivity

Direction selectivity has been recorded from retinal ganglion cells in several different species, including goldfish, frog and toad, turtle, pigeon, cat and rabbit [17]. Barlow and Hill [18] reported that some ganglion cells in the rabbit responded vigorously when successive stimuli were presented in one direction across their receptive fields (the preferred direction), and decreased their activity when movement was in the opposite direction (the null direction for that ganglion cell). The receptive field is that region of the visual field to which the ganglion cell responds. It is generally concentric - encompassing up to eight degrees of visual angle [19]. Barlow et al. [19,20] proposed that direction selectivity was the result of an inhibitory mechanism that vetoed responses in the null direction. Current thought on the mechanism for direction selectivity in the vertebrate retina (shown in Figure 2) remains based on the convergence excitation and inhibition at the input to the ganglion dendrite [6,22]. The functional components of the mechanism involve only the two different types of amacrine cells: one inhibiting, and the other exciting the direction sensitive ganglion cells. The two types are arranged spatially so that a moving image activates first one then the other. The preferred direction requires activation of excitation in advance of inhibition, while the null direction requires the converse.

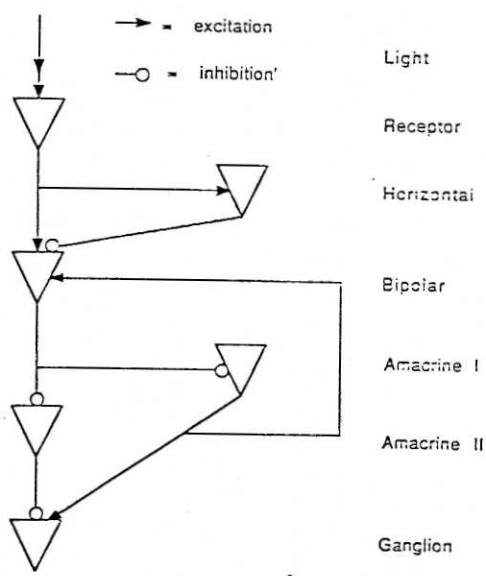

Figure 1. Model of motion analysis subnetwork.

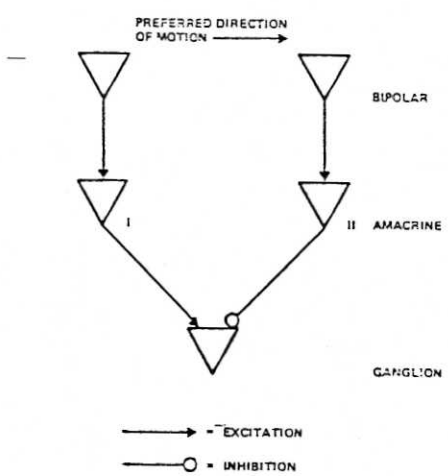

Figure 2. Mechanism of direction selectivity in retina.

2. SYNOPSIS OF THE MODEL

There is more than one way to connect processing elements in a model retina to achieve direction selectivity. In this paper, we will describe and contrast two of our more successful variations. One method involves inhibition of bipolar to ganglion transmission (I-variant), the other involves facilitation of bipolar to ganglion transmission (F-variant).

The basic retinal model for motion processing is a feed-forward sparsely interconnected neural network, based on the models shown in Figures 1 and 2. The connection patterns for the I and F variations of this network are shown in Figures 3a and 3b respectively, and described below. The numbers of elements in the networks can be arbitrary, dependent only on the size and resolution of the digitized image, and on the ability of the computing machine to process the information in the required time. However, the numbers of the different types of elements maintain fixed proportions to the total. There are six different types of elements, roughly analogous to receptor, horizontal, bipolar, amacrine I and II, and ganglion cells of the biological retina. Elements of like type are assembled into layers. The layers are connected by delay lines. Activity originating in the receptors percolates through the retina, delayed by one time constant (t) at some connections as noted below. The time constant in the current implementation is defined by the program cycle time.

The receptive field is divided into sectors by the convergence of an area of bipolars on A-I amacrines and of A-II amacrines on ganglion elements. As a minimum, we use four sectors which divide the visual field into four equal quadrants.

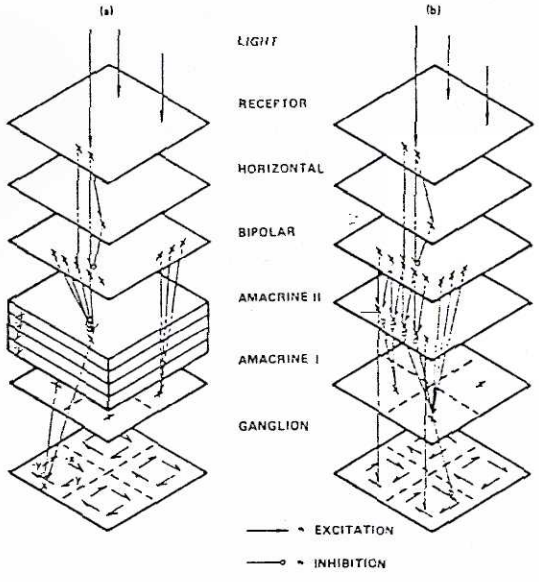

Figure 3. Two variations on the mechanism of direction selectivity. (a) shows the use of persistent lateral inhibition to block conduction in the null direction. (b) shows the use of persistent lateral excitation to facilitate the conduction in the preferred direction.

2.1. Receptor elements

The receptor (R) matrix is represented by gray-scale values which can originate from an image simulator or a frame grabber that has digitized television camera images, or a matrix from some other sensor. Simulator and frame grabber values range between 0 and 256. Higher numbers are associated with brighter light. These values are forwarded to horizontal and bipolar matrices in columnar pathways.

2.2. Horizontal elements

Horizontal (H) elements receive input without delay from the nearest receptor located immediately above.

$$Hij(t) = Rij(t) \tag{1}$$

where i indexes the position on the X axis, and j indexes the position on the Y axis of a Cartesian map of the receptor surface. Horizontal element output is forwarded to the bipolar element located immediately below, after a delay of one cycle.

2.3. Bipolar elements

Bipolar (B) elements compare the inputs from local receptor and horizontal elements, passing on the positive value of the difference. The choice of differencing is not critical for the performance of the model. Bipolar output could be made contingent upon only increases in light intensity (R-H), upon only decreases in light intensity (H-R), or upon change in either direction, derived by taking the absolute value of the difference (|R-H|).

$$Bij(t) = Hij(t-1) - Rij(t) \tag{2}$$

$$Bij(t)out = \begin{cases} Bij(t) & \text{if } Bij(t) > \phi \\ \phi & \text{if } Bij(t) \leqslant \phi \end{cases} \tag{3}$$

The local change in light intensity is transferred to the two types of amacrine elements. The bipolar output is passed to the A-I amacrine element in its local sector and also to the A-II amacrine elements through a connection matrix that determines sensitivity to direction of intensity change across the receptor layer.

2.4. Amacrine elements

Type A-I amacrine (AI) elements integrate input only from bipolar elements in the local sector and send output to adjust thresholds of sector ganglion elements. A percentage (g) of A-I activity persists.

$$AI_{(t)} = g \times AI_{(t+1)} + \Sigma\, Bij(t)\ out \tag{4}$$

It is the connectivity and functions of the A-II amacrines that contribute to the variation in our model of direction selectivity. In the I-variant, there is persistent inhibition in the null direction. Bipolar input accumulates and persists in A-II amacrine elements which then inhibit and block bipolar conduction to ganglion elements in the null direction. In the I-variant, each ganglion element is associated with a unique field of A-II amacrine elements (or dendritic regions of a few large amacrine elements) that store the inhibition. In the F-variant, persistent excitation in the preferred direction is used. There is only one field of amacrine elements and this is shared by each of the four direction-sensitive ganglion elements in a sector. Excitation is distributed and stored horizontally in advance of movement in the preferred direction and used to facilitate the bipolar to ganglion transmission. The differences in the two models will now be

described separately, beginning with the model using persistent inhibition.

Type A-II amacrine (AII) elements sum bipolar output within small receptive fields of a sector with any residual inhibition (with a persistence factor of e). The receptive field of an A-II amacrine element is limited to bipolars lying on one axis of the X-Y plane and behind its overlying bipolar relative to the direction selectivity for that plane of elements. The bipolar's influence on the amacrine elements is subject to 1/d, where d is the horizontal distance between them. In practice, we have limited d to the value of 3.

$$AII_{Dij(t)} = e \times AII_{Dij(t-1)} + \sum_{d} (Bij \pm d(t)\ out) \div d \qquad (5)$$

where D is the direction selectivity. D determines which index (i or j) to increment (+) or decrement (-). The residual inhibition has an exponential decline and so is maximal with recent movement in the null direction.

Output to a direction-sensitive ganglion element is the bipolar activity that exceeds the local residual inhibition from the A-II amacrine associated with that direction.

$$AII_{Dij(t)\ out} = pos\ (Bij(t)\ out - AII_{Dij(t-1)}) \qquad (6)$$

In the variation using persistent excitation, type A-II amacrine (AII) elements also accumulate bipolar output with a persistence factor of e,

$$AII_{ij(t)} = e \times AIIij(t-1) + Bij(t)\ out \qquad (7)$$

but, the horizontal spread of AII potentials creates a facilitatory gate for the transmission of new bipolar activity on to the ganglion element. The sensitivity of this gate is itself modulated by a portion (f) of the sector's A-I amacrine activity.

$$AII_{Dij(t)\ out} = (AII_{ij \pm 1(t-1)} \times Bij(t)) \div (f \times AI) \qquad (8)$$

A recent history of activity from bipolar elements on one side biases the amacrine element's sensitivity to activity from bipolar elements on the other side.

2.5. Ganglion elements

In both variations, there are four ganglion (G) elements per sector, each defining a preferred direction (D). Each ganglion element integrates activity from all of the bipolar elements in its sector with mediation by the A-II amacrine elements, and compares that sum with a portion (h) of the accumulated potential on the A-I amacrine. Lateral inhibition between complementary ganglion elements of a sector (left vs. right, and up vs. down) prevent contradictory responses even in conditions of high noise.

$$G_D = \Sigma AII_{Dij\ out} - \Sigma AII_{-Dij\ out} \qquad (9)$$

$$G_{D\ out} = \begin{cases} 1 \text{ if } G_D > h \times AI \\ 0 \text{ if } G_D \leq h \times AI \end{cases} \qquad (10)$$

The activity state of the ganglion element is set to 1 if the ganglion potential exceeds its threshold (the ganglion element fires), otherwise it is set to zero. The activity states of the ganglion elements code the network's decisions about the certainty of coherent movement in a sector of the visual field. Increasing the A-I amacrine element potential is equivalent to raising the criterion for certainty. Ganglion element activity in a sector provides location information to the resolution of the size of the sector. The speed of movement is coded in the pulse frequency of the ganglion element output. The direction of movement in a sector is determinable from the relative firing rates of the ganglion elements since they code speed of movement along orthogonal X and Y axes.

3. SIMULATION HARDWARE

The model was implemented in the C programming language. Simulations were performed on a Sun Microsystems workstation. An IBM/PC-AT was used with a frame-grabber to study digitized video images. The IBM-PC/AT insured compatibility with the IBM-PC/AT bus used by the laboratory's free-swimming underwater vehicle (EAVE-WEST). The field-of-view of the video camera was approximately 32 degrees. This provided two degrees of visual angle between the receptors using a 16 by 16 receptor field. The digitized frame of 512 by 512 was sampled at 32 pixel intervals to produce the smaller array. The IBM-PC/AT update rate with the I-variant was 2.5 frames per second while that of the F-variant was 4 frames per second. Comparable simulations on the Sun ran eight times as fast.

4. BEHAVIOR OF THE MODEL

Criteria for adequate behavior were 1) rapid fading of a stationary image, 2) increase in the output pulse rate proportional to the speed of image movement, 3) increase in X/Y output asymmetry proportional to the direction of image movement off the diagonal, and 4) unambiguous response to movement with signal- to-noise ratios (S/N) of 5 or better. The two variations of the model were tested with A-I persistence set to 0.5, A-I to ganglion and A-I to A-II gains set to 0.1, and A-II persistence set to 0.7 in the I-variant and to 0.5 in the F-variant.

4.1. Insensitivity to stationary images

In the present model, the horizontal elements guarantee that the image will disappear if stationary for two or more program cycles. Because the bipolars respond to the difference between the horizontals and receptors, only positive intensity differences are passed on to the amacrines. However, the model generally works well for both increases and decreases in light intensity if either brightening or dimming detection is used. This is because an inverse image trail accompanies any movement (except an expanding light region with dimming detection or an expanding dark region with brightening detection). The motion sensitivity of the model is similar to the performance of the artificial retina developed by Mead and Mahowald [23]. They were able to implement in VLSI the first three types of retinal cells. Our model extends this processing through to the ganglion cell layer providing information on speed and direction of movement.

4.2. Speed sensitivity

In the absence of noise, the model reliably produced an output each time the image moved from one receptor to another. Slowly moving images simply persisted on receptors and horizontals and disappeared from bipolars until a new receptor was crossed and stimulated by a change in brightness. The integrated output of the ganglion elements was related to the speed of image movement between two limits. The lower limit resulted from the loss of A-II activity that blocked or gated the bipolar output to the ganglion layer, governed by the A-II persistence. The upper limit was due to the sampling rate of the system. The I- variant was more successful at following slowly moving images (<< 0.1 degree of visual angle per second) because A-II persistence could be set at a much higher level than in the F-variant. Under high-noise conditions, the residual excitation of the F-variant acted like an indiscriminate sieve that passed most activity on through to the ganglion layer.

4.3. Direction sensitivity

Images that were moved on either the horizontal or vertical axes generated unambiguous responses from detectors aligned with the movement. Off-axis movement resulted in appropriate combinations of vertical and horizontal responses. The mechanism responsible for this effect was the relative number of receptors crossed by the moving image per unit of time. Under some conditions, however, the direction of movement defined by the relative ganglion output was orthogonal to the orientation of the leading edge of the image and bore no relationship to the true direction of movement of the center of mass of the moving object. The conditions under which this occurred, such as when the object

was much larger than the visual field, prevented the determination of the object's center of gravity.

4.4. Noise immunity

The effects of noise on the ability of the retinal model to track a moving image were explored by varying the S/N in simulations. The S/N was defined by the ratio of the contrast difference between the moving image and the mean background intensity, and the rms of the background at each sample. Background noise was random in both temporal and spatial domains but its variance was consistent over time. Figure 4 provides the error rate as a function of S/N for the two variations of the model. An error was defined as either an omission of the appropriate response or as the commission of an inappropriate response. The target was a homogeneous line extending the full width of the visual field and moving at the maximum velocity. The error curve describes a sigmoidal relationship to S/N. In the I-variant, errors were negligible until the S/N was reduced to 4. Then the error rate accelerated to asymptote at 75%. In the F-variant, the error curve demonstrated greater accuracy than the I-variant with higher levels of noise. The F-variant was 95% accurate at a S/N ratio of 3. The maximum error rate of 75% was reached by both variations of the model at a S/N near 1. Random firings of the 4 ganglion elements would guarantee the maximum error rate.

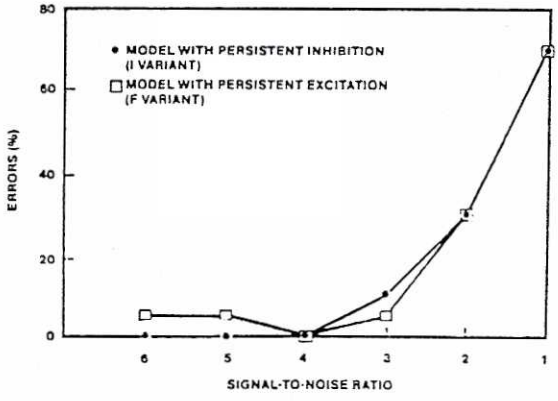

Figure 4. Errors in ganglion element output as a function of noise.

5. THE CONTEXT OF VISUAL MOTION ANALYSIS

The success of our model must be assessed by its ability to extract relevant information from the environment. This information will be used by additional processing stations to generate an appropriate motor response. Through simple reflex connections between movement detectors and motor controllers, the vehicle could seek out and orient to man-made objects such as anchor chains or pilings. Collisions with either stationary or moving objects could be avoided using the same information. The reflexes that steer a vehicle toward some feature in the visual field could be inverted to steer the vehicle away from the feature. Additional processing stations would be tasked with making the decision to approach or to avoid. One criterion for such a decision may be the velocity of closure.

5.1. Image movement caused by motion of vehicle

Movement of the vehicle in a stationary environment will cause all of the features to move on the receptor surface. If the vehicle is moving horizontally relative to a vertical line, a large response will be generated in the vertical detectors, while vertical movement of the vehicle against the same vertical line will allow it to go virtually undetected. Appropriately connected to motor controllers, the detector output will tend to keep the most significant features in the center of the visual field. This response is similar by design to the optokinetic reflex of insects that keeps them moving in straight lines and compels them to orient to high contrast edges [1]. This behavior is extremely useful for underwater tasks such as cable tracking.

5.2. Image movement caused by motions of both object and vehicle

Independent movement of objects in the visual field of a moving vehicle can occur in a tracking scenario. If there are no stationary objects, then the problem of tracking is simplified to that of orienting to a moving target from a stationary platform, or to a stationary target from a moving platform, for either condition will result in similar effects in the movement analysis network. However, if both the vehicle and the target are moving in a field of stationary objects, some method must be applied to filter the motion information due to the vehicle's movement. Since collision avoidance will likely be required, this information cannot simply be discarded. Rather, the unique motions of the target must be identified. The amphibian appears to sidestep this problem by remaining motionless, or, if the environment persists in moving, by stabilizing the background movement with an opposing movement of the eyes [24]. An alternative to the amphibian strategy is to have a secondary motion processing station respond to the change in detector output such that the continuous motion information can be attributed to vehicle movement while deviations limited to some sectors could be attributed to target movement. For example, decelerations in all sectors indicate that the vehicle itself is slowing down, while a deceleration in one sector indicates that a target has moved. Information from other sensors such as Doppler sonar, accelerometer, or altimeter can also be used to assess vehicle movement and assist in visual fixations.

5.3. Velocity sensitivity

In the absence of noise, the present model codes velocity of an object moving across the visual field by the frequency of action potentials generated at the ganglion elements. The maximum velocity to which the model can encode is limited by the program cycle (or update) time when running on a serial machine. This is currently four frames per second on an IBM-PC/AT. With the 16 by 16 receptor array and a 32-degree field-of-view, this translates to 8 degrees of visual angle per second. For comparison, the maximum velocity that can be tracked by a cell in the visual cortex is about 25 degrees visual angle per second [25]. In an implementation where it is possible to process the receptor input in parallel, output will still be proportional to velocity, but the maximum encodable velocity will be limited only by the throughput speed of the system. At velocities below the maximum for the model, the output over time is proportional to the velocity. The system tracks slow moving objects in the absence of noise down to velocities in the range of 0.1 degree visual angle per second. For comparison, the lower limit of a cortical cell to track a moving image is about one minute of visual angle per second [26].

6. BIOLOGICAL FIDELITY OF THE MODEL

Of the two variations of the model that we have described, the I-variant is more aligned with known biological mechanisms than the F-Variant. Several studies have shown that inhibition is necessary for the null response from direction-sensitive ganglion cells [13,27]. The F-Variant, however, may model the effects of the central reafferent control over the retinal motion analysis. Activity originating in the optic tectum is known to flow back over the optic nerve to disinhibit amacrine cells and enhance the ganglion cell response [28]. In our model, the facilitation due to excitation moving in advance of the image reduced errors in the model's determination of image direction under moderate noise conditions. Thus, a central prediction or expectation of the direction of movement can, through reafference and the mechanism of facilitation demonstrated here, improve the perception of that movement. While our model digresses from available neurophysiological data, we offer it as a working solution to the problem of visual motion information for guidance of autonomous vehicles, rather than as a hypothesis of biological mechanisms. We do suggest that the number of parsimonious solutions is limited, and because nature tends to exploit simple solutions, some insight into unknown biological mechanisms may be gained through this type of exploration.

7. REFERENCES

1. R. Wehner, "Spatial vision in arthropods," in Vision in Invertebrates, H. Autrum, ed., Handbook of Sensory Physiology, VII/6c, Springer-Verlag, Berlin (1981).

2. R. Held, H.W. Leibowitz, and H.-L. Teuber, eds., Perception, Handbook of Sensory Physiology, VIII, Springer-Verlag, Berlin (1978).

3. W.R. Levick and E.R. Dvorak, "The retina-from molecules to networks," Trends in Neurosciences, 9, 181-185 (1986).

4. R.H. Masland, "The functional architecture of the retina," Scientific American, 255, 102-111 (1986).

5. P. Sterling, M. Freed, and R.G. Smith, "Microcircuitry and functional architecture of the cat retina," Trends in Neurosciences, 9, 186-192 (1986).

6. J.E. Dowling, The Retina: An Approachable Part of the Brain Belknapp Press, Cambridge, MA (1987).

7. D.C. van Essen and J.H.R. Maunsell, "Hierarchical organization and functional streams in the visual cortex," Trends in Neurosciences, 6, 1-6 (1983).

8. M.S. Livingstone, "Art, illusion and the visual system," Scientific American, 258, 78-85 (1988).

9. J. Richter and S. Ullman, "A model for the temporal organization of X- and Y- type receptive fields in the primate retina," Biological Cybernetics, 43, 127-145 (1982).

10. P. Sterling, "Microcircuitry of the cat retina," Annual Review of Neuroscience, 6, 149-185 (1983).

11. F.S. Werblin, "The control of sensitivity in the retina," Scientific American, 228, 71-79 (1973).

12. M. Tauchi and R.H. Masland, "The shape and arrangement of the cholinergic neurons in the rabbit retina," Proceedings of the Royal Society of London, B, 223, 101-119 (1984).

13. J.H. Caldwell, N.W. Daw, and H.J. Wyatt, "Effects of picrotoxin and strychnine on rabbit retinal ganglion cells," Journal of Physiology, 276, 277- 298 (1978).

14. E.V. Famiglietti, Jr., "On and off pathways through amacrine cells in mammalian retina: The synaptic connections of "starburst" amacrine cells," Vision Research, 23, 1265-1268 (1983).

15. E.V. Famiglietti, Jr. and H. Kolb, "Structural basis for on- and off- center responses in retinal ganglion cells," Science, 194, 193-195 (1976).

16. R.H. Masland, J.W. Mills, and C. Cassidy, "The functions of acetylcholine in the rabbit retina," Proceedings of the Royal Society of London, B, 223, 121-139 (1984).

17. O.-J. Grusser and U. Grusser-Cornehls, "Neuronal mechanisms of visual movement perception and some psychophysical and behavioral correlations," in Central Processing of Visual Information. R. Jung, ed., Handbook of Sensory Physiology, VII/3B. Springer-Verlag, Berlin, 333-429 (1973).

18. H.B. Barlow and R.M. Hill, "Selective sensitivity to direction of motion in ganglion cells of the rabbit's retina," Science, 139, 412-414 (1963).

19. S.W. Kuffler and J.G. Nicholls, From Neuron to Brain, Sinauer, Sunderland, MA (1977).

20. H.B. Barlow, R.M. Hill, and W.R. Levick, "Retinal ganglion cells responding selectively to direction and speed of image motion in the rabbit," Journal of Physiology, 173, 377-407 (1964).

21. H.B. Barlow and W.R. Levick, "The mechanism of directionally selective units in rabbit's retina," Journal of Physiology, 178, 477-504 (1965).

22. C. Koch, T. Poggio, and V. Torre, "Computations in the vertebrate retina: Gain enhancement, differentiation and motion discrimination," Trends in Neurosciences, 9, 204-211 (1986).

23. C.A. Mead and M. Mahowald, "A silicon model of early visual processing," Neural Networks, 1, 91-97 (1988).

24. J.Y. Lettvin, H.R. Maturana, W.S. McCulloch, and W.H. Pitts, "What the frog's eye tells the frog's brain," Proceedings of the IRE, 47, 1940-1959 (1959).

25. G.H. Henry, "Neural processing in cat striate cortex," IEEE Transactions on Systems, Man, and Cybernetics, SMC-13, 888-900 (1983).

26. A.W. Goodwin, G.H. Henry, and P.O. Bishop, "Direction selectivity of simple striate cells: Properties and mechanisms," Journal of Neurophysiology, 38, 1500-1523 (1975).

27. M. Ariel and A.R. Adolph, "Neurotransmitter inputs to directionally sensitive turtle retinal ganglion cells," Journal of Neurophysiology, 54, 1123- 1143 (1985).

28. R.W. Rodieck, The Vertebrate Retina: Principles of Structure and Function, W.H. Freeman and Co., San Francisco (1973).